NJC

Accepted Manuscript

This is an *Accepted Manuscript*, which has been through the Royal Society of Chemistry peer review process and has been accepted for publication.

Accepted Manuscripts are published online shortly after acceptance, before technical editing, formatting and proof reading. Using this free service, authors can make their results available to the community, in citable form, before we publish the edited article. We will replace this *Accepted Manuscript* with the edited and formatted *Advance Article* as soon as it is available.

You can find more information about *Accepted Manuscripts* in the Information for Authors.

Please note that technical editing may introduce minor changes to the text and/or graphics, which may alter content. The journal's standard Terms & Conditions and the Ethical guidelines still apply. In no event shall the Royal Society of Chemistry be held responsible for any errors or omissions in this *Accepted Manuscript* or any consequences arising from the use of any information it contains.

ROYAL SOCIETY OF CHEMISTRY

www.rsc.org/njc

Journal Name

ARTICLE

A BODIPY/Pyridine conjugate for reversible fluorescence detection of gold(III) ions

Received 00th January 20xx,
Accepted 00th January 20xx

DOI: 10.1039/x0xx00000x

www.rsc.org/

Muhammed Üçüncü, Erman Karakuş and Mustafa Emrullahoğlu*

We designed a "turn-on" type fluorescent probe based a BODIPY-Pyridine conjugate which exhibits high selectivity towards Au(III) ions and, also responds to changes in the pH within the acidic pH range. The probe offers features such as rapid response time, a low detection limit, high sensitivity and selectivity. The detection of Au(III) is recognized by a distinct change in the emission intensity which relies on a reversible "ligand to ion" binding mechanism. We have also documented the utility of the probe for the quantification of gold ion residues in synthetic end products prepared via gold catalysis

Introduction

During the last decade, the catalytic properties of gold have attracted a surge of attention in the field of synthetic chemistry. Ionic species of gold, in contrary to elemental gold, have the exceptional capability to activate unsaturated bonds (e.g. alkyne) towards the addition nucleophiles.[1-5] Besides their peerless catalytic activities, gold ions present interesting biological properties. For a long time, certain drugs based on various gold ion complexes have been used in the treatment of diseases including rheumatic arthritis, cancer, asthma, and HIV.[6-8] In contrast to their beneficial roles in disease treatment, the intake of gold ions can also cause toxicity to the living organisms because of the possibility to interact with biomolecules such as enzymes and DNA. Numerous scientific studies have established the detrimental effects of gold species on vital human organs. For instance, the intake of $AuCl_3$ causes damage to kidneys, liver, and the peripheral nervous system.[9-11]

The potential health hazard associated with gold species pushes the demand for developing trustable and efficient methods to trace levels of gold species existing in synthetic chemicals prepared via gold catalysis.

Trace metal analysis relying on fluorescence techniques are very popular nowadays.[12-16] In contrast to the traditional instrumental techniques, fluorescence-based techniques have many preferable advantages such as low cost, simplicity, high sensitivity and reproducibility. Several gold ion selective molecular sensors utilizing various fluorophore units- including rhodamine,[17-21] BODIPY,[22-25] fluorescein,[26,27] naphthalimide,[28,29] and coumarin[30] dyes- have been developed over the last years.[31,32] The great majority of those sensors present in the literature are based on irreversible chemical events, which take advantage of the alkynophilic behaviour of gold species. In general, the fluorophore core being integrated with a gold ion specific reactive unit (i.e. alkyne), transforms the action of gold ions into a fluorescent signal output either through a change in fluorescence wavelength or a change in fluorescence intensity.[33] Notably, one chronic issue in reaction-based gold ion sensing is the potential of other alkynophilic metal species to interfere with detection of gold ions. Thus, new sensing strategies utilizing alternative recognition events are needed to be developed in order to improve the general shortcomings of reaction based sensing strategies.

In this regard, molecular sensors relying on reversible ion-dipole interactions appear as good alternatives to reaction-based molecular sensors. Interestingly, however, molecular sensors operating reversibly towards gold ions are extremely scarce, most predominantly due to the challenge in design and synthesis.[34]

Herein, we present the design, synthesis and spectral properties of **BOD-Pyr**, a novel turn-on type fluorescent chemosensor that allows both Au^{3+} and H_3O^+ ions to be detected on the basis of reversible ion-dipole interactions. Knowing the capability of pyridine to act as a ligand for ionic gold species, we envisioned that a pyridine motif, when integrated to a fluorophore core, could act as a specific recognition motif for gold ions. Several Bodipy-pyridine conjugates have been reported in the literature which respond to changes in pH or to certain metal species such as Cu^{2+} and Hg^{2+}.[35-37]

With all these in mind, we designed a molecular structure, which comprises a BODIPY dye as a fluorophore unit and a pyridylethenyl motif as the recognition site. The BODIPY core was the fluorophore of choice owing to its exceptional

[a] Department of Chemistry, Faculty of Science, İzmir Institute of Technology, Urla, 35430, Izmir, Turkey E-mail: mustafaemrullahoglu@iyte.edu.tr

†Electronic Supplementary Information (ESI) available: Absorbance and fluorescence data and all experimental procedures. See DOI: 10.1039/x0xx00000x

photophysical properties such as high photo stability, high fluorescence quantum yield, robustness towards light and chemicals, and long emission/absorption wavelength.[38-41]

Results and Discussions

BOD-Pyr was prepared by the synthetic route outlined in Scheme 1. First, a Vilsmeier Haack's formylation reaction of **BODIPY-1** gave **BODIPY-2**,[42] which in the final step was treated with an appropriate Wittig reagent to give exclusively the *E*-isomer of the title compound in a reasonable yield of ca. 56% (Scheme 1). The chemical structure of **BOD-Pyr** was clearly confirmed by performing NMR spectroscopy and HRMS analysis.

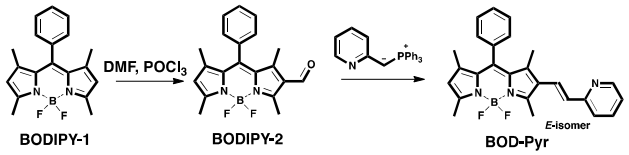

Scheme 1 Synthetic Route for **BOD-Pyr**.

Au^{3+} Sensing Properties of BOD-Pyr

The photophysical behaviour of **BOD-Pyr** in response to a series of metal species was carried out by both UV–vis absorption and fluorescence spectroscopy. We commenced our investigation by first determining the optimum conditions for the recognition of Au^{3+} ions. A variety of solvent combinations involving EtOH-H_2O, DMF-H_2O, and CH_3CN-H_2O (Fig. S1, ESI†) were screened. Furthermore, the ratio of water in the semi-aqueous environment and the effect of pH on the sensing process were carefully investigated. Eventually, the optimum condition for the sensing process was established as 0.1 M phosphate buffer/EtOH (pH 7.0, v/v, 1:1) with 10 µM dye concentration (Figs. S2,S3, ESI†).

The spectral changes of **BOD-Pyr** in the absence and presence of Au^{3+} ions are displayed in Fig. 1. As shown, free **BOD-Pyr** exhibits a faint fluorescence emission cantered at 591 nm. (Φ_F=0.044). However, the addition of Au^{3+} (6 equiv.) to **BOD-Pyr** results in an observable enhancement of the emission intensity together with a slight blue shift in the emission wavelength (λ_{em}=577 nm) in a very short time (30 sec.) (Fig. S4 ESI†). This spectral behaviour of **BOD-Pyr** was suggested to be due to the complexation of $AuCl_3$ with the lone pair electrons of the pyridylethenyl unit, which terminates the overall PET-quenching process.

Importantly, neither the absorption nor the fluorescence emission wavelength of **BOD-Pyr** was affected by changing the polarity of the sensing media which indicates that **BOD-Pyr** has indeed no solvatochromic behaviour.

The selectivity profile of **BOD-Pyr** was surveyed by screening the spectral response towards metal species including Zn^{2+}, Cd^{2+}, Ba^{2+}, Cu^{2+}, Li^{+}, K^{+}, Ni^{2+}, Cr^{2+}, Mg^{2+}, Fe^{3+}, Pb^{2+}, Hg^{2+}, Co^{2+}, Ag^{+} and Au^{+}. Delightfully, no significant changes were measured in the presence of other metal species. Only the addition of Au^{3+} and, to a lesser extent the addition of Au^{+} resulted in an increase of fluorescence at 577 nm, which obviously implied the high selectivity of **BOD-Pyr** to gold ions (Fig. S8, ESI†). Fortunately, Hg^{2+} and Pd^{2+}, being the most competitive metal ions in the detection of gold species did not result in any spectral change.

In order to assess the interference of other metal ions we explored the fluorescence response in the presence of other metal ions. As shown in Fig. S9 (ESI†), the response of **BOD-Pyr** towards Au^{3+} was not affected in the presence of other competitive metal species. These results established that **BOD-Pyr** can properly detect gold ions in the mixtures of other related species.

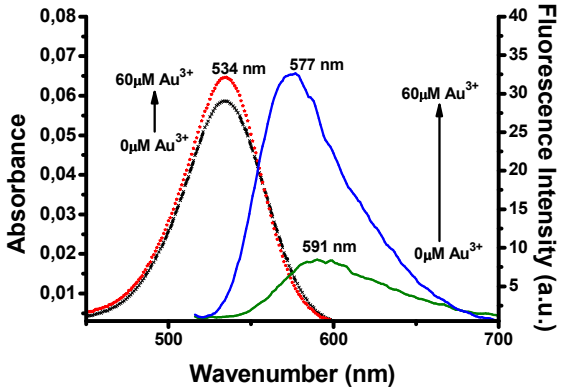

Fig. 1 Absorbance spectra of **BOD-Pyr** (10µM) in the absence (black dot-line) and presence (red dot-line) of 6 equiv. (60µM) of Au^{3+} and fluorescence spectra of **BOD-Pyr** (10µM) in the absence (green line) and presence (blue line) of 6 equiv. (60µM) of Au^{3+} in 0.1 M phosphate buffer/EtOH (pH 7.0, v/v, 1:1).

We further investigated the binding ability of **BOD-Pyr** to Au^{3+} by performing a fluorescence titration experiment (Fig. 2). The emission intensity reached its maximum when 6 equiv. of Au^{3+} was added and the stoichiometry of the sensing event was established by following the Benesi-Hildebrand method and Job's plot analysis. In addition, there was a good linear relationship between fluorescence intensity and the equivalency of Au^{3+} ions (0.2 to 0.7 equivalent of Au^{3+}) (Fig. S10, ESI†). From this data the detection limit of **BOD-Pyr** was evaluated as 4.0 µM. A straight line was obtained from the plot of $\ln[(F-F_0)/(F_{max}-F)]$ against $\ln[Au^{3+}]$ and the related binding constant was determined as 4.9 x 10^4 M^{-2}. Moreover, the Job's plot analysis supported a 2:1 stoichiometry for the complexation. Despite great efforts, we failed to grow a single crystal of the binding complex suitable for XRD analysis in order to confirm the binding stoichiometry.

The specific binding of Au^{3+} to the pyridine ligand could be clearly followed by the aid of ^{1}H-NMR spectroscopy. Upon binding of $AuCl_3$ with **BOD-Pyr**, the pyridine ring protons (H_b, H_c and H_d) of the binding complex dramatically shifted to a higher frequency (downfield shift), consistent with coordination of nitrogen to $AuCl_3$ (Fig. 2b and Fig. S15 ESI†).

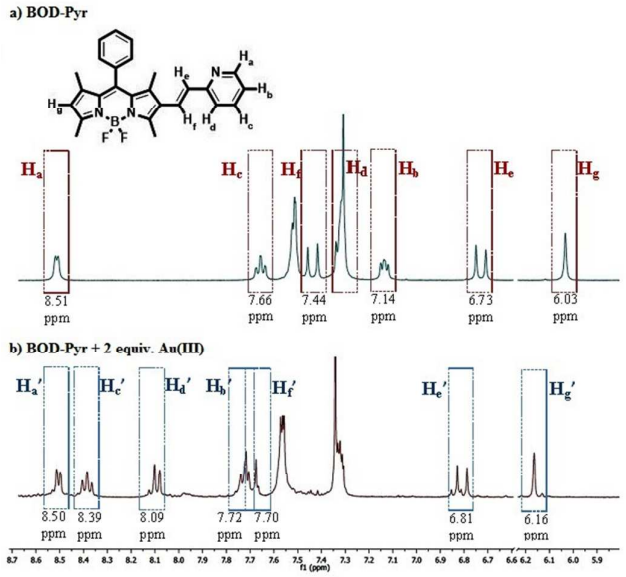

Fig. 2 a) Partial ^{1}H NMR spectrum of **BOD-Pyr** and b) **BOD-Pyr** +$AuCl_3$ (2 equiv)

Further experiments revealed that the binding ability of **BOD-Pyr** to Au^{3+} could be dramatically improved in a non-aqueous sensing media. For example in DCE the binding constant was evaluated to be 1.8 x 10^5 M^{-2}, which was visibly greater than, that measured in the aqueous media (Fig.S14, ESI†).

In a non-aqueous sensing media, where the effect of solvation is minimized, the complexation of Au^{3+} to the Bodipy-pyridine conjugate gave a 20-fold fluorescence enhancement, which is visibly greater than the fluorescence increase observed in aqueous media. Similar to the measurements carried out in aqueous conditions, the fluorescence titration profile of **BOD-Pyr** with Au^{3+} in non-aqueous media showed a linear relationship for a concentration range of 0.05-1.0 μM (Fig. S16, ESI†). Notably, the detection limit of **BOD-Pyr** was significantly improved to nanomolar levels (63 nm, S/N > 3). However, it is worth mentioning here that, despite the improved sensitivity, the selectivity towards Au^{3+} dramatically decreased in non-aqueous media.

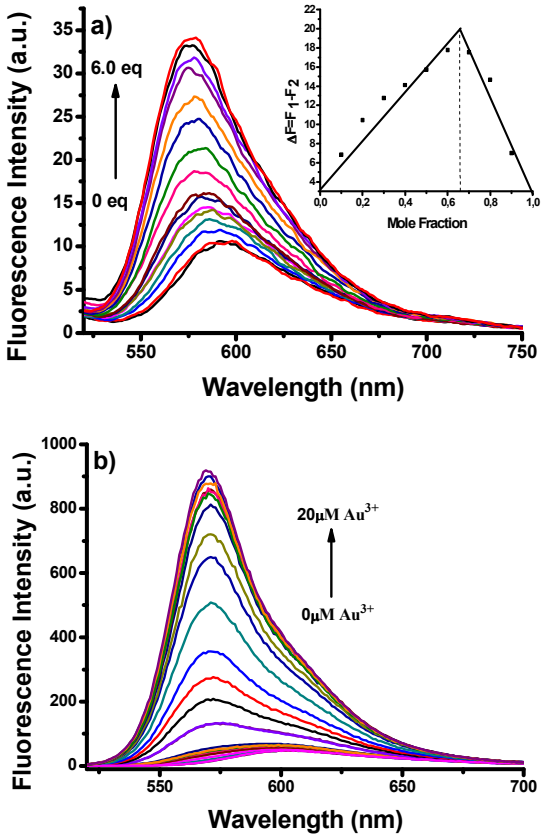

Fig. 3 Fluorescence spectra of **BOD-Pyr** (10μM) in the presence of increasing concentrations of Au^{3+} (a) (0-60 μM, 0-6 equiv.) in 0.1 M phosphate buffer/EtOH (pH 7.0, v/v, 1:1) (λ_{exc}=500 nm at 25°C) and (b) (0-20μM, 0-2 equiv.) in DCE. Inset: The Job plot analysis between **BOD-Pyr** and Au^{3+}. The total concentration of **BOD-Pyr** and Au^{3+} was kept constant at 20 μM.

The sensing mechanism of the probe was envisioned to be reversible. To get insight into whether the sensing mechanism is reversible or not, an excess amount of CN^- ion (NaCN, 6.0 equiv) was introduced into the solution including 10 μM dye and 6.0 equivalents of Au^{3+} (0.1 M phosphate buffer/EtOH (pH 7.0, v/v, 1:1). As shown in Fig. S12 (ESI†), the fluorescence intensity of the probe solution was immediately reduced by the addition of CN^- which proofs the reversibility of recognition process (Scheme 2).

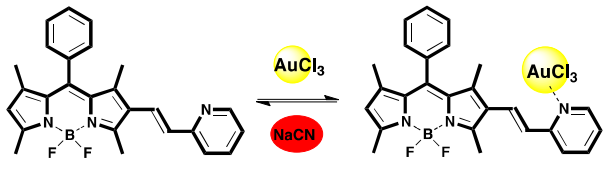

Scheme 2 Reversible interaction of **BOD-Pyr** with Au^{3+}

Response of BOD-Pyr toward pH changes

In addition to being exceptionally selective towards Au^{3+} ions, **BOD-Pyr** is also sensitive to changes in pH within the acidic pH range. Free **BOD-Pyr**, which exhibits a faint fluorescence emission at 591 nm in pH range of 7-12, gave immediately a strong emission band at 564 nm upon protonation of pyridylethenyl moiety (Fig. 4b). As the pH of solution decreased from 7.0 to 2.0, concomitantly the emission intensity increased by 18-fold. The quantum yield of **BOD-Pyr** at pH=2.0, was determined to be 0.39 by using rhodamine 6G (Φ_F=0.95 in ethanol) as a standard dye.

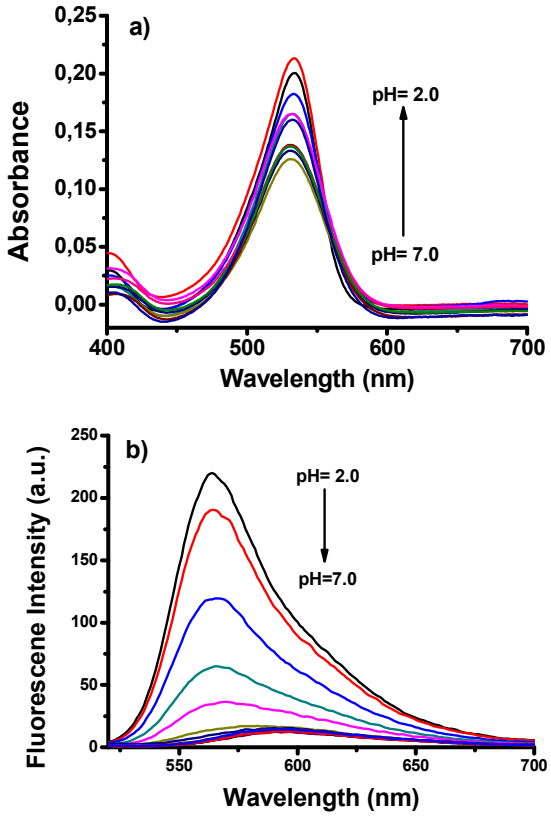

Fig. 4 (a) Absorbance and (b) Fluorescence spectra of **BOD-Pyr** (10 μM) in 0.1 M phosphate buffer/EtOH (v/v, 1:1) at various pH values (2.0-7.0) (λ_{exc}=500 nm, 25 °C).

As for the gold sensing process, **BOD-Pyr** operates in a reversible manner towards the detection of hydronium ions (Scheme 3). The reversible interaction between the **BOD-Pyr** and H_3O^+ was confirmed by the addition of OH^- ions to the acidified probe solution (**BOD-Pyr** + H_3O^+) which resulted in a sharp decrease in emission intensity.

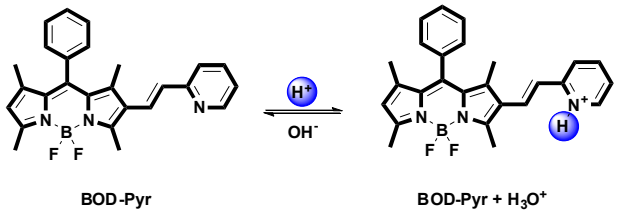

Scheme 3 Reversible protonation of **BOD-Pyr**.

Regeneration of fluorescence was again possible by introducing H_3O^+ ions into the solution. Obviously, the "off-on" switching ability of the system proved the reversibility of the process. In addition, the acidity constant pK_a of the probe was established by using a Henderson–Hasselbalch equation (Fig. 5b). A linear fit was obtained within the range of pH from 2.0 to 6.0 and pK_a value was calculated as 3.06 ± (0.14). All these results indicate that, **BOD-Pyr** can also be utilized on demand as a "turn-on" fluorescent probe for monitoring acidity changes within the pH range of 7.0-2.0.

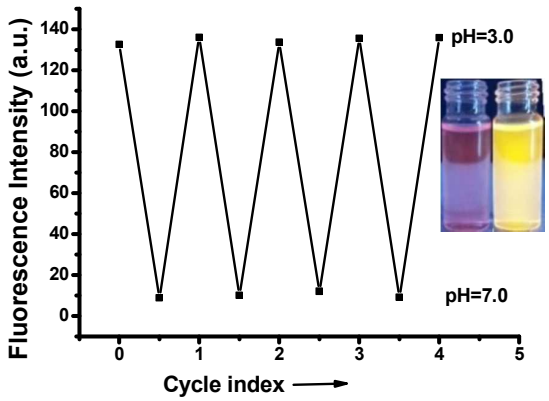

Fig. 5 pH reversibility study of **BOD-Pyr** (10μM) between pH 7.0 and 3.0 in water/EtOH (v/v, 1:1) (λ_{exc}=500 nm, λ_{em}=564 nm, 25 °C). Inset: Fluorescence photographs of **BOD-Pyr** at pH 7.0 (left) and 3.0 (right) under illumination with 365 nm light.

Quantitative detection of residual Au^{3+}

In order to assess whether **BOD-Pyr** could be applied to monitoring residual Au^{3+} ions in a synthetic end-product we performed a known chemical transformation utilizing $AuCl_3$ as the active catalyst.[43] To this end, a propargylic amide derivative in dichloromethane was rapidly transformed to its Oxazole derivative under the catalysis of $AuCl_3$ (10 mol%) (Scheme 4).

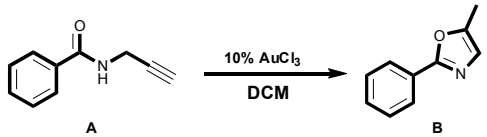

Scheme 4 $AuCl_3$ catalysed cyclization reaction of propargyl amide

The crude product of the chemical reaction was subjected to chromatographic purification using silica as the stationary phase and dichloromethane as an eluent. A defined amount of the purified sample (2 mg) was added to the solution of **BOD-Pyr** (10 µM in 0.1 M phosphate buffer/EtOH (pH 7.0, v/v, 1:1). Immediately, a distinct change in colour and fluorescence could be monitored in the probe solution indicating the presence of gold species in the solution. This observation was in consistent with previous literature reports, where others and we have proven that a synthetic end product may still contain residues of the metal catalyst even after chromatographic purification.

By the aid of fluorescence measurements the gold content in the sample solution was measured to be 1.8 x 10^{-8} mol mg^{-1} based on a standard calibration curve (Fig. S16, ESI†). This result was also consistent with that obtained by inductively coupled plasma-mass spectrometry (ICP-MS) analysis (1.27 x 10^{-8} mol mg^{-1}). With this experiment we unambiguously confirmed the viability of **BOD-Pyr** for quantitative gold analysis.

Conclusions

To close, we have constructed a dual responsive fluorescent chemosensor for the rapid detection of gold species and, also for monitoring the changes in acidity (pH=2-7). This novel chemosensor (**BOD-Pyr**) comprises a pyridylethenyl unit as a recognition site and a BODIPY core as a fluorophore unit. The sensing mechanism of **BOD-Pyr** is based on selective binding of gold ions to the pyridyl-nitrogen atom which is recognized by a distinct change in the emission intensity. Importantly, **BOD-Pyr** represents a rare example of a fluorescent probe that operates "reversibly" towards gold species. As a practical application we have successfully documented the utility of **BOD-Pyr** for the quantification of gold ion residues in synthetic chemicals that were prepared via gold catalysis.

Experimental Section

General Methods

All reagents were purchased from commercial suppliers (Aldrich and Merck) and they were used without further purification. ^{1}H NMR and ^{13}C NMR were measured on a Varian VNMRJ 400 Nuclear Magnetic Resonance Spectrometer. Bruker MALDI-TOF-TOF Mass Spectrometer was used for mass spectrometry analysis. UV absorption spectra were obtained on Shimadzu UV-2550 Spectrophotometer. Fluorescence measurements were performed by using Varian Cary Eclipse Fluorescence spectrophotometer. Samples were contained in 10.0 mm path length quartz cuvettes (2.0 mL volume). Upon excitation at 500 nm, the emission spectra were integrated over the range 520 nm to 750 nm. The slit width was 5 nm for both excitation and emission. Melting points were determined by using an Electrothermal Melting Point Apparatus 9200. The pH was recorded by HI-8014 instrument (HANNA). All measurements were conducted at least in triplicate.

Synthesis of BOD-Pyr

To a solution of **Bodipy-2** (100 mg, 0.285 mmol) in dioxane (10 mL) was added triphenyl(2-pyridylmethyl)phosphonium chloride hydrochloride (389 mg, 0.896 mmol). Then, 250 µl of triethyl amine was added drop by drop and the resultant solution was stirred at room temperature for overnight. After the reaction completed, the solution was concentrated in vacuum and extracted three times with dichloromethane. The organic layer was dried over sodium sulfate and concentrated under reduced pressure. The resultant residue was purified by silica gel column chromatography (hexane / ethyl acetate (8/1)) to afford **BOD-Pyr** as green solid (68.1mg, 56% yield). Mp: 267-269 ^{o}C. ^{1}H NMR (400 MHz, $CDCl_3$) δ: 8.56 (d, J= 4.0 Hz, 1H), 7.62 (d_t, J= 8.0, 1.6 Hz 1H), 7.52-7.50 (m, 3H), 7.46 (s, 1H), 7.32-7.29 (m, 2H), 7.28 (s, 1H), 7.12-7.09 (m, 1H), 6.72 (d, J= 16.0 Hz, 1H), 6.01 (s, 1H), 2.76 (s, 3H), 2.58 (s, 3H), 1.51 (s, 3H), 1.38 (s, 3H). ^{13}C NMR (100 MHz, $CDCl_3$) δ: 156.3, 155.9, 154.9, 149.6, 143.8, 141.8, 139.3, 136.5, 135.0, 132.0, 131.0, 129.5, 129.2, 129.1, 128.1, 127.8, 123.9, 121.8, 121.8, 14.7, 14.5, 14.1, 12.9. Calcd. for $C_{26}H_{24}BF_2N_3$: 427.203 $[M]^+$, Found: 428.244 $[M+H]^+$.

Acknowledgements

We thank İzmir Institute of Technology (İZTECH) and TUBİTAK for financial support.

Notes and references

1 I. Braun, A. M. Asiri and A. S. K. Hashmi, *ACS Catal.*, 2013, **3**, 1902.
2 Z. Li, C. Brouwer and C. He, *Chem. Rev.*, 2008, **108**, 3239.
3 A. Arcadi, *Chem. Rev.*, 2008, 108, 3266.
4 A. S. K. Hashmi and M. Rudolph, *Chem. Soc. Rev.*, 2008, **37**, 1766.
5 N. Krause and C. Winter, *Chem. Rev.*, 2011, **111**, 1994.
6 C. F. Shaw III, *Chem. Rev.*, 1999, **99**, 2589.
7 I. Ott, *Coord. Chem. Rev.*, 2009, **253**, 1670.
8 M. Navarro, *Coord. Chem. Rev.*, 2009, **253**, 1619.
9 C. M. Goodman, C. D. McCusker, T. Yilmaz and V. M. Rotello, *Bioconjugate Chem.*, 2014, **15**, 897.
10 A. Habib and M. Tabata, *J. Inorg. Biochem.*, 2004, **98**, 1696.
11 W. D. Block and E. L. Knapp, *JPET*, 1945, **83**, 275.
12 X. Li, X. Gao, W. Shi and H. Ma, *Chem. Rev.*, 2014, **114**, 590.
13 K. P. Carter, A. M. Young and A. E. Palmer, *Chem. Rev.*, 2014, **114**, 4564.
14 X. Chen, T. Pradhan, F. Wang, J. S. Kim and J. Yoon, *Chem. Rev.*, 2012, **112**, 1910.
15 X. Su and I. Aprahamian, *Chem. Soc. Rev.*, 2014, **43**, 1963.
16 Z. Guo, S. Park, J. Yoon and I. Shin, *Chem. Soc. Rev.*, 2014, **43**, 16.
17 M. J. Jou, X. Chen, K. M. K. Swamy, H. N. Kim, H.-J. Kim, S. G. Lee and J. Yoon, *Chem. Commun.*, 2009, 7218.
18 O. A. Egorova, H. Seo, A. Chatterjee and K. H. Ahn, *Org. Lett.*, 2010, **12**, 401.
19 Y. K. Yang, S. Lee and J. Tae, *Org. Lett.*, 2009, **11**, 5610.

20 L. Yuan, W. Lin, Y. Yang and J. Song, *Chem. Commun.*, 2011, **47**, 4703.
21 M. Emrullahoğlu, E. Karakuş and M. Üçüncü, *Analyst*, 2013, **138**, 3638.
22 J.-B. Wang, Q.-Q. Wu, Y.-Z. Min, Y.-Z. Liu and Q.-H. Song, *Chem. Commun.*, 2012, **48**, 744.
23 E. Karakuş, M. Üçüncü and M. Emrullahoğlu, *Chem. Commun.*, 2014, **50**, 1119.
24 M. Üçüncü and M. Emrullahoğlu, *Chem. Commun.*, 2014, **50**, 5884.
25 M. Üçüncü, E. Karakuş and M. Emrullahoğlu, *Chem.–Eur. J.*, 2015, DOI: 10.1002/chem.201502411.
26 H. Seo, M. E. Jun, O. A. Egorova, K. H. Lee, K. T. Kim and K. H. Ahn, *Org. Lett.*, 2012, **14**, 5062.
27 N. Y. Patil, V. S. Shinde, M. S. Thakare, P. H. Kumar, P. R. Bangal, A. K. Barui and C. R. Patra, *Chem. Commun.*, 2012, 48, 11229.
28 M. Dong, Y.-W. Wang and Y. Peng, *Org. Lett.*, 2010, **12**, 5310.
29 J. Y. Choi, G.-H. Kim, Z. Guo, H. Y. Lee, K. M. K. Swamy, J. Pai, S. Shin, I. Shin and J. Yoon, *Biosens. Bioelectron.*, 2013, **49**, 438.
30 J. H. Do, H. N. Kim, J. Yoon, J. S. Kim and H.-J. Kim, *Org. Lett.*, 2010, **12**, 932.
31 Z. Öztaş, M. Pamuk and F. Algi, *Tetrahedron*, 2013, **69**, 2048.
32 Y. Yang, C. Yin, F. Huo and J. Chao, *RSC Adv.*, 2013, **3**, 9637.
33 S. Singha, D. Kim, H. Seo, S. W. Cho and K. H. Ahn, *Chem. Soc. Rev.*, 2015 DOI: 10.1039/C4CS00328D.
34 J. Wang, W. Lin, L. Yuan, J. Song and W. Gao, *Chem. Commun.*, 2011, **47**, 12506.
35 E. Deniz, G. C. Isbasar, Ö. A. Bozdemir, L. T. Yıldırım, A. Siemiarczuk and E. U. Akkaya, *Org. Lett.*, 2008, **10**, 3401.
36 S. Wagner, K. Brödner, B. A. Coombs and U. H. F. Bunz, *Eur. J. Org. Chem.*, 2012, 2237.
37 L. Zhou, C.–C. Zhu, Y.–S. Xue, W.–J. He, H.–B. Du, X.–Z. You and Y.–Z. Li, *Inorg. Chem. Commun.*, 2013, **35**, 355.
38 N. Boens, V. Leen and W. Dehaen, *Chem. Soc. Rev.*, 2012, **41**, 1130.
39 R. Ziessel, G. Ulrich and A. Harriman, *New J. Chem.*, 2007, **31**, 496.
40 A. Loudet and K. Burgess, *Chem. Rev.*, 2007, **107**, 4891.
41 G. Ulrich, R. Ziessel and A. Harriman, *Angew. Chem., Int. Ed.*, 2008, **47**, 1184.
42 M. Isik, T. Ozdemir, I. S. Turan, S. Kolemen and E. U. Akkaya, *Org. Lett.*, 2013, **15**, 216.
43 A. S. K. Hashmi, J. P. Weyrauch, W. Frey and J. W. Bats, *Org. Lett.*, 2004, **6**, 4391.

Graphical Abstract:

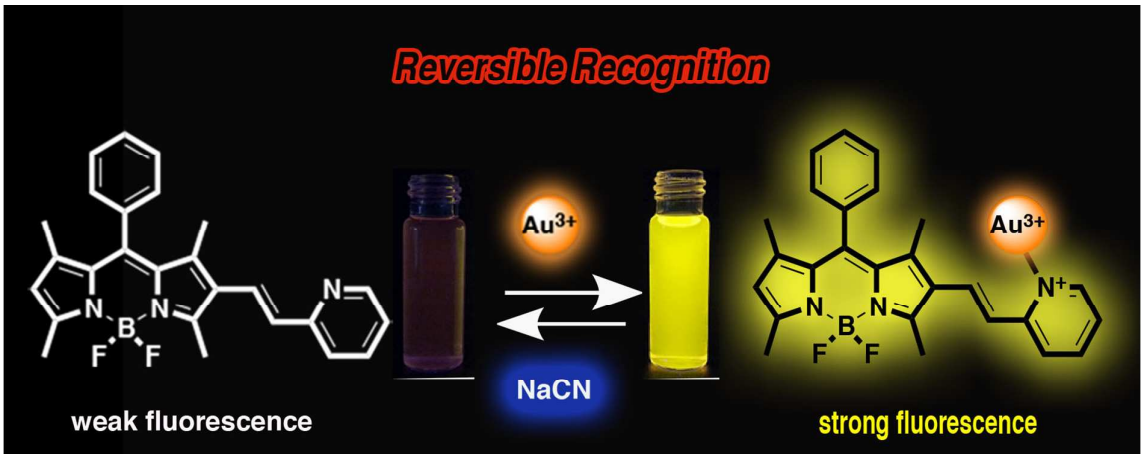

A rare example of a fluorescent probe for reversible detection of gold ions